Large Deformations of a Whirling Elastic Cable

By C. Y. Wang and Layne T. Watson

TR 90-19

Large Deformations of a Whirling Elastic Cable

C.-Y. Wang
Departments of Mathematics and Mechanical Engineering
Michigan State University
East Lansing, MI 48824 USA

Layne. T. Watson
Department of Computer Science
Virginia Polytechnic Institute & State University
Blacksburg, VA 24061 USA

Abstract. The large deformation of a whirling elastic cable is studied. The ends of the cable are hinged but otherwise free to translate along the rotation axis. The nonlinear governing equations depend on a rotation-elasticity parameter J. Bifurcation about the straight, axially rotating case occurs when $J \geq n\pi$. Perturbation solutions about the bifurcation points and matched asymptotic solutions for large J are found to second order. Exact numerical solutions are obtained using quasi-Newton and homotopy methods.

1. Introduction and formulation. The whirling of long, slender materials occurs in the manufacture and winding of cables and strings. It is also important in the study of deployable, flexible space structures, such as the rotation of long cables connecting two satellites (e.g., [1, 2]). This paper is an in-depth analysis of such a flexible rotating cable or slender rod.

Consider an originally straight cable of length ℓ rotating axially with angular velocity Ω. The ends of the cable are hinged to the rotation axis. When Ω is larger than some critical value, the cable may deform due to centrifugal forces as shown in Figure 1a. For relatively stiff cables the situation is very similar to the whirling of shafts, the linear stability of which has been studied much earlier (e.g., [3, 4]). For our problem, the finite deformation characteristics are needed.

Let the deformed cable be contained in a rotating x', y' plane. Let the origin be at one end with the x'-axis along the rotation axis. Consider a small elemental segment ds' whose arc length distance is s' from the origin (Figure 1b). The force acting on this segment is $F' - u'$, where F' is the vertical force experienced at the ends and u' is the net centrifugal force from the origin to s'.

$$u' = \int_0^{s'} \rho \Omega^2 y' \, ds', \tag{1}$$

where ρ is the mass per unit length of the cable. A moment balance on ds' gives

$$m = m + dm + (F' - u')ds' \cos\theta. \tag{2}$$

Since the cable is thin, the local moment m is proportional to the local curvature and deformation is due mostly to bending,

$$m = EI\frac{d\theta}{ds'}. \tag{3}$$

Normalize the variables as follows:

$$x = \frac{x'}{\ell}, \quad y = \frac{y'}{\ell}, \quad s = \frac{s'}{\ell}, \quad F = \frac{\ell^2 F'}{EI}, \quad u = \frac{u'}{\rho\Omega^2\ell^2}. \tag{4}$$

Eqs. (1–3) yield

$$\frac{d^2\theta}{ds^2} + \left(F - J^4 u\right)\cos\theta = 0, \tag{5}$$

$$\frac{du}{ds} = y, \qquad u(0) = 0, \tag{6}$$

where $J \equiv \Omega^{1/2}\ell(\rho/EI)^{1/4}$ is an important nondimensional parameter representing the relative importance of rotation to flexural rigidity. The Cartesian coordinates are related by

$$\frac{dx}{ds} = \cos\theta, \qquad \frac{dy}{ds} = \sin\theta. \tag{7}$$

The boundary conditions are

$$x(0) = y(0) = 0, \qquad \frac{d\theta}{ds}(0) = 0, \tag{8}$$

$$y(1) = 0, \qquad \frac{d\theta}{ds}(1) = 0. \tag{9}$$

Eqs. (5–9) are to be solved for given J. There are six boundary conditions for the fifth degree differential equations plus one unknown constant F.

2. Analysis of the bifurcation neighborhood. For small θ, u, y, Eqs. (5–7) linearize to

$$\frac{d^2\theta}{ds^2} + F - J^4 u = 0, \qquad \frac{du}{ds} = y, \qquad \frac{dy}{ds} = \theta. \tag{10}$$

Eliminate u, y and let $\theta \approx \phi$. The eigenvalue problem is

$$\frac{d^4\phi}{ds^4} - J^4\phi = 0 \tag{11}$$

with the boundary conditions

$$\frac{d\phi}{ds}(0) = \frac{d^3\phi}{ds^3}(0) = \frac{d\phi}{ds}(1) = \frac{d^3\phi}{ds^3}(1) = 0. \tag{12}$$

The general solution to Eq. (11) is

$$\phi = c_1\sin(Js) + c_2\cos(Js) + c_3\sinh(Js) + c_4\cosh(Js). \tag{13}$$

The boundary conditions give

$$c_1 = c_3 = 0, \qquad c_2\sin J = c_4\sinh J = 0. \tag{14}$$

Since the coefficients in Eq. (13) are not all zero, the eigenvalues are

$$J = n\pi, \qquad n = 1, 2, 3, \ldots \tag{15}$$

and the eigenfunctions are

$$\phi = \cos(n\pi s), \qquad n = 1, 2, 3, \ldots \tag{16}$$

Observe that the cable is approximately sinusoidal in shape and crosses the rotation axis at the points $s = 0, 1/n, 2/n, \ldots, 1$, where the curvatures are also zero. Thus it suffices to consider only the $n = 1$ case. The higher modes can always be constructed from the $n = 1$ case by multiplying all lengths by a factor of $1/n$. This characteristic also holds for the original nonlinear problem.

In order to investigate the bifurcation properties near $J = \pi$, set

$$J = \pi + \epsilon^2, \qquad \theta = \epsilon\theta_0 + \epsilon^3\theta_1 + \mathcal{O}(\epsilon^5) \tag{17}$$

$$u = \epsilon u_0 + \epsilon^3 u_1 + \mathcal{O}(\epsilon^5), \qquad F = \epsilon\alpha_0 + \epsilon^3\alpha_1 + \mathcal{O}(\epsilon^5), \tag{18}$$

$$x = x_0 + \epsilon^2 x_1 + \mathcal{O}(\epsilon^4), \qquad y = \epsilon y_0 + \epsilon^3 y_1 + \mathcal{O}(\epsilon^5). \tag{19}$$

Eqs. (5–9) yield the successive equations

$$\frac{d^2\theta_0}{ds^2} + \alpha_0 - \pi^4 u_0 = 0, \qquad \frac{du_0}{ds} = y_0, \tag{20}$$

$$\frac{dx_0}{ds} = 1, \qquad \frac{dy_0}{ds} = \theta_0, \tag{21}$$

$$\frac{d\theta_0}{ds}(0) = \frac{d\theta_0}{ds}(1) = u_0(0) = x_0(0) = y_0(0) = y_0(1) = 0, \tag{22}$$

$$\frac{d^2\theta_1}{ds^2} + \alpha_1 - 4\pi^3 u_0 - \pi^4 u_1 - \frac{\theta_0^2}{2}(\alpha_0 - \pi^4 u_0) = 0, \tag{23}$$

$$\frac{du_1}{ds} = y_1, \qquad \frac{dy_1}{ds} = \theta_1 - \frac{\theta_0^3}{6}, \tag{24}$$

$$\frac{dx_1}{ds} = -\frac{1}{2}\theta_0^2, \tag{25}$$

$$\frac{d\theta_1}{ds}(0) = \frac{d\theta_1}{ds}(1) = u_1(0) = x_1(0) = y_1(0) = y_1(1) = 0. \tag{26}$$

The solution to the zeroth order problem Eqs. (20–22) is

$$\theta_0 = c\phi = c\cos(\pi s), \tag{27}$$

$$\alpha_0 = \pi^2 c, \qquad u_0 = \frac{c}{\pi^2}(1 - \cos(\pi s)), \tag{28}$$

$$x_0 = s, \qquad y_0 = \frac{c}{\pi}\sin(\pi s). \tag{29}$$

Here c is an undetermined amplitude, characteristic of eigenvalue problems. To determine c, the next order perturbation is studied.

Differentiate Eq. (23) twice and eliminate u_1, y_1 by Eq. (24). The result is

$$\frac{d^4\theta_1}{ds^4} - \pi^4\theta_1 = A(s), \tag{30}$$

$$\begin{aligned} A(s) &= 4\pi^3\theta_0 - \frac{\pi^4}{6}\theta_0^3 - \frac{1}{2}\frac{d^2}{ds^2}\left[\theta_0^2\frac{d^2\theta_0}{ds^2}\right] \\ &= c\pi^3\left(4 - \pi c^2/2\right)\cos(\pi s) - \frac{7}{6}c^3\pi^4\cos(3\pi s). \end{aligned} \tag{31}$$

Since the function A is proportional to $\cos(\pi s)$ and $\cos(3\pi s)$, the particular solution for θ_1 is proportional to $s\sin(\pi s)$ and $\cos(3\pi s)$ respectively, the latter satisfying all the boundary conditions since it is an eigenfunction ϕ. However, the term $s\sin(\pi s)$ could not be made to satisfy the boundary conditions, even with the aid of the homogeneous solutions. Thus the function A could not have contained terms proportional to $\cos(\pi s)$. In other words, the integrability condition is

$$c = \sqrt{\frac{8}{\pi}}. \tag{32}$$

Absorb the homogeneous solution for θ_1 into θ_0 since it has the same form. Thus Eq. (30) gives

$$\theta_1 = -\frac{7\sqrt{2}}{30\pi\sqrt{\pi}}\cos(3\pi s). \tag{33}$$

From Eqs. (24, 25),

$$\alpha_1 = \frac{59}{10}\sqrt{2\pi}, \tag{34}$$

$$u_1 = \frac{1}{\pi^3}\sqrt{\frac{2}{\pi}}\left(\frac{1}{10}\cos(3\pi s) + 2\cos(\pi s) - \frac{21}{10}\right), \tag{35}$$

$$x_1 = -\frac{2}{\pi^2}\left(\pi s + \frac{1}{2}\sin(2\pi s)\right), \tag{36}$$

$$y_1 = -\frac{1}{\pi^2}\sqrt{\frac{2}{\pi}}\left(\frac{3}{10}\sin(3\pi s) + 2\sin(\pi s)\right). \tag{37}$$

The normalized force at the ends is

$$\begin{aligned} F &= \epsilon\alpha_0 + \epsilon^3\alpha_1 + \mathcal{O}(\epsilon^5) \\ &= (2\pi)^{3/2}(J-\pi)^{1/2}\left[1 + \frac{59}{20\pi}(J-\pi) + \cdots\right]. \end{aligned} \tag{38}$$

The maximum lateral displacement occurs at $s = 1/2$:

$$\begin{aligned} b &= \epsilon y_0(1/2) + \epsilon^3 y_1(1/2) + \mathcal{O}(\epsilon^5) \\ &= (2/\pi)^{3/2}(J-\pi)^{1/2}\left[1 - \frac{17}{20\pi}(J-\pi) + \cdots\right]. \end{aligned} \tag{39}$$

The maximum curvature or normalized moment is

$$M = -\frac{d\theta}{ds}(1/2) = -\epsilon\frac{d\theta_0}{ds}(1/2) - \epsilon^3\frac{d\theta_1}{ds}(1/2) + \mathcal{O}(\epsilon^5)$$
$$= 2\sqrt{2\pi}(J-\pi)^{1/2}\left[1 - \frac{7}{20\pi}(J-\pi) + \cdots\right]. \tag{40}$$

The distance between ends is

$$a = x_0(1) + \epsilon^2 x_1(1) + \mathcal{O}(\epsilon^4)$$
$$= 1 - \frac{2}{\pi}(J-\pi) + \cdots. \tag{41}$$

3. Asymptotic analysis for large J. Large J means large rotation rate, long length, high density or low rigidity. We expect the cable to be hairpin-shaped with the maximum curvature occurring at $s = 1/2$. Set

$$J^4 \equiv \frac{2}{\delta^3} \gg 1. \tag{42}$$

Eq. (5) becomes singular:

$$\delta^3\theta''(s) + 2\big[u(1/2) - u(s)\big]\cos\theta = 0, \tag{43}$$

where

$$F = \frac{2}{\delta^3}u(1/2), \qquad \theta(1/2) = \theta''(1/2) = 0. \tag{44}$$

The method of matched asymptotic expansions will be used. For the interior region, where $0 < 1/2 - s = \mathcal{O}(1)$, the cable is almost perpendicular to the rotation axis. Perturb about this state as follows:

$$\theta = \frac{\pi}{2} + \delta H_1(s) + \delta^2 H_2(s) + \cdots, \tag{45}$$
$$u = \frac{s^2}{2} + \delta U_1(s) + \delta^2 U_2(s) + \cdots, \tag{46}$$
$$x = \delta X_1(s) + \delta^2 X_2(s) + \cdots, \tag{47}$$
$$y = s + \delta Y_1(s) + \delta^2 Y_2(s) + \cdots. \tag{48}$$

Substituting into Eqs. (43, 6, 7) and utilizing the fact that $u(0) = y(0) = x(0) = 0$ gives that the first and second order corrections are all zero. For the boundary layer region where $1/2 - s = \mathcal{O}(\delta)$ set

$$s = \frac{1}{2} - \delta t, \qquad t = \mathcal{O}(1), \tag{49}$$
$$\theta = \phi_0(t) + \delta\phi_1(t) + \mathcal{O}(\delta^2), \tag{50}$$
$$u = \frac{1}{8} - \delta v_1(t) - \delta^2 v_2(t) + \mathcal{O}(\delta^3), \tag{51}$$
$$x = \delta\xi_1(t) + \delta^2\xi_2(t) + \mathcal{O}(\delta^3), \tag{52}$$
$$y = \frac{1}{2} - \delta\eta_1(t) + \mathcal{O}(\delta^3). \tag{53}$$

Here the constant terms of Eqs. (50, 52) are from matching with the interior solution. The general matching condition is

$$W_{\text{interior}}\Big|_{s\to 1/2-\delta t} = W_{\text{boundary layer}}\Big|_{t\to\infty} \tag{54}$$

where W represents θ, u, x, or y. Substitution of Eqs. (49–53) into Eqs. (43, 6, 7) yields the successive equations

$$\frac{dv_1}{dt} = \frac{1}{2}, \tag{55}$$

$$\frac{d^2\phi_0}{dt^2} + 2\left[v_1(t) - v_1(0)\right]\cos\phi_0 = 0, \tag{56}$$

$$\frac{d\eta_1}{dt} = \sin\phi_0, \tag{57}$$

$$\frac{d\xi_1}{dt} = -\cos\phi_0, \tag{58}$$

$$\frac{dv_2}{dt} = -\eta_1, \tag{59}$$

$$\frac{d^2\phi_2}{dt^2} + 2\left[v_2(t) - v_2(0)\right]\cos\phi_0 - 2\left[v_1(t) - v_1(0)\right]\phi_1\sin\phi_0 = 0, \tag{60}$$

$$\frac{d\xi_2}{dt} = \phi_1\sin\phi_0. \tag{61}$$

The boundary conditions are $\phi_0(0) = \phi_1(0) = 0$. Using the matching condition, as $t \to \infty$, $\phi_0 \to \pi/2$, $\phi_1 \to 0$, $v_1 \to t/2$, $v_2 \to -t^2/2$, $\eta_1 \to t$, $\xi_1 \to 0$, $\xi_2 \to 0$. The solution to Eq. (55) is

$$v_1 = \frac{t}{2}. \tag{62}$$

Eq. (56) becomes

$$\frac{d^2\phi_0}{dt^2} + t\cos\phi_0 = 0, \tag{63}$$

which with the boundary conditions constitutes a two-point boundary value problem. This problem can be solved by simple shooting: guess a value for $\phi_0'(0)$ and integrate Eq. (63) using a Runge-Kutta algorithm; then adjust the initial value and repeat until the right hand boundary condition is satisfied. This one-dimensional shooting yields $\phi_0'(0) = 1.096606$. Similarly Eqs. (57–61) are successively integrated with the results $\eta_1(0) = 0.60127$, $\xi_1(0) = 1.2175$, $v_2(0) = 0.2934$, $\phi_2'(0) = -0.5570$, $\xi_2(0) = 0.8248$. Thus

$$F = \frac{2}{\delta^3}\left[\frac{1}{8} - \delta v_1(0) - \delta^2 v_2(0) + \cdots\right] = J^4\left[\frac{1}{8} - 0.2934\left(\frac{2}{J^4}\right)^{.2/3} + \mathcal{O}(J^{-4})\right], \tag{64}$$

$$M = \frac{1}{\delta}\left[\phi_0'(0) + \delta\phi_1'(0) + \cdots\right] = \left(\frac{J^4}{2}\right)^{1/3}\left[1.0966 - 0.5570\left(\frac{2}{J^4}\right)^{1/3} + \mathcal{O}(J^{-8/3})\right], \tag{65}$$

$$a = 2\left[\delta\xi_1(0) + \delta^2\xi_2(0) + \cdots\right] = 2\left(\frac{2}{J^4}\right)^{1/3}\left[1.2175 + 0.8248\left(\frac{2}{J^4}\right)^{1/3} + \mathcal{O}(J^{-8/3})\right], \tag{66}$$

$$b = \frac{1}{2} - \delta\eta_1(0) + \cdots = \frac{1}{2} - 0.60127\left(\frac{2}{J^4}\right)^{1/3} + \mathcal{O}(J^{-8/3}). \tag{67}$$

4. Numerical integration. Numerical integration of the original equations is necessary if $J - \pi$ is neither large nor small. Define $w = \big(F,\ \theta(0)\big)$ and let $\theta(s;w)$, $u(s;w)$, $x(s;w)$, $y(s;w)$ be the solution of the initial value problem given by Eqs. (5–8) and using w. The original two-point boundary value problem is equivalent to solving the nonlinear system of equations

$$G(w) = \Big(\frac{d\theta}{ds}(1;w), \quad y(1;w) \Big) = 0. \tag{68}$$

Algorithms for solving the nonlinear system Eq. (68) typically require partial derivatives $\partial G_i/\partial w_j$. Since $G(w)$ is defined implicitly by the solution of a nonlinear ordinary differential equation, these partials cannot be found analytically. Finite difference approximations could be used, but for the same amount of work as a central difference, the partials can be calculated to the same accuracy as $G(w)$. This is done as follows: let

$$Z = \left(\theta, \theta', u, x, y, \frac{\partial\theta}{\partial w_j}, \frac{\partial\theta'}{\partial w_j}, \frac{\partial u}{\partial w_j}, \frac{\partial x}{\partial w_j}, \frac{\partial y}{\partial w_j} \right) \tag{69}$$

and consider the first order system

$$\begin{aligned}
Z_1' &= Z_2, \\
Z_2' &= -\big(F - J^4 Z_3\big) \cos Z_1, \\
Z_3' &= Z_5, \\
Z_4' &= \cos Z_1, \\
Z_5' &= \sin Z_1, \\
Z_6' &= Z_7, \\
Z_7' &= \big(F - J^4 Z_3\big) Z_6 \sin Z_1 - \big(\delta_{1j} - J^4 Z_8\big) \cos Z_1, \\
Z_8' &= Z_{10}, \\
Z_9' &= -Z_6 \sin Z_1, \\
Z_{10}' &= Z_6 \cos Z_1,
\end{aligned} \tag{70}$$

with the initial condition

$$Z(0) = (w_2, 0, 0, 0, 0, \delta_{2j}, , 0, 0, 0, 0)\,. \tag{71}$$

By solving this system twice, for $j = 1$ and $j = 2$, all the partial derivatives $\partial G_i/\partial w_j$ can be calculated, with an accuracy determined by the accuracy of the numerical solution to the above initial value problem.

The nonlinear system Eq. (68) is solved by a combination of quasi-Newton methods [5] and globally convergent homotopy methods [6, 7]. Very briefly, the strategy is to use the globally convergent and robust homotopy method to obtain a few solutions, and then use the inexpensive (but only locally convergent) quasi-Newton method to generate other solutions as J is slowly varied.

5. Results and discussion. Figure 2 shows the normalized maximum moment M, occurring at the midpoint, as a function of J. The perturbation solution about the bifurcation point is accurate (within 5% error) for J less than 3.8. Similarly the asymptotic solution for large J is accurate for $J > 4.5$. Figure 3 shows the maximum force occurring at the ends. The approximate solutions compare fairly well in their respective ranges of validity. Figure 4 shows that the maximum width a decreases and the maximum height b increases with J after bifurcation. Figure 5 shows some cable configurations for different values of J. The cable is straight and rotates axially if $J \leq \pi$. The boundary layer character becomes evident for large J. These figures are important in the design of rotating cables. If the cable has no flexural rigidity, $EI \to 0$ and $J \to \infty$. The chain would double up into a thin hairpin and rotate perpendicular to the rotation axis.

This paper has used both direct numerical integration and perturbation methods to obtain the solution. While direct numerical integration is more accurate, it does not show parametric variations. For example, $M \sim (J - \pi)^{1/2}$ for small $J - \pi$ and $M \sim J^{4/3}$ for large J can not be easily predicted by numerical integration. Also, if J is large, the term J^4 causes Eq. (4) to be extremely stiff near $s = 1/2$, resulting in the direct numerical solutions becoming either expensive or inaccurate. However, numerical integration was used to solve Eqs. (56–61). These integrations are universal and independent of J, i.e., they can be performed once and for all.

The problem considered here is somewhat similar to the free rotation of an elastic ring about a diameter [8]. There are, however, marked differences. The rotating ring does not bifurcate from a critical rotation number J and thus the force and moment characteristics are quite different. The procedure described here for the higher order perturbations about the bifurcation point and the higher order large J asymptotic analysis should also be interesting to engineers and applied mathematicians.

6. Acknowledgement. The work of L. T. Watson was supported in part by DOE Grant DE-FG05-88ER25068, NASA Grant NAG-1-1079, NSF Grant CTS-8913198, and AFOSR Grant 89-0497.

7. References.

[1] Ebner, S. G.: Deployment dynamics of rotating cable-connected space stations. *J. Spacecraft and Rockets* **7**, 1274–1275 (1970).

[2] Singh, R. B.: Three dimensional motion of a system of two cable-connected satellites in orbit. *Astro. Acta* **18**, 301–308 (1973).

[3] Dunkerley, S.: On the whirling and vibration of shafts. *Phil. Trans. Roy. Soc. London* **A185**, 279–360 (1894).

[4] Love, A. E. H.: *A Treatise on the Mathematical Theory of Elasticity.* 4th ed., Dover, New York, 442–443 (1944).

[5] Moré, J. J., Garbow, B. S., and Hillstrom, K. E.: *User Guide for MINPACK-1.* ANL-80-74, Argonne National Laboratory, Argonne, IL (1980).

[6] Watson, L. T., Billups, S. C., and Morgan, A. P.: HOMPACK: A suite of codes for globally convergent homotopy algorithms. *ACM Trans. Math. Software* **13**, 281–310 (1987).

[7] Watson, L. T.: A globally convergent algorithm for computing fixed points of C^2 maps. *Appl. Math. Comput.* **5**, 297–311 (1979).

[8] Wang, C.-Y., and Watson, L. T.: Free rotation of a circular ring about a diameter. *J. Appl. Math. Phys.* **34**, 13–24 (1983).

Figure Captions

Figure 1. a) The coordinate system. b) The elemental length.

Figure 2. Normalized maximum moment as a function of J. Dashed lines are approximations.

Figure 3. Normalized force as a function of J.

Figure 4. Maximum width a and maximum height b.

Figure 5. Cable configurations for various J.

Fig 1

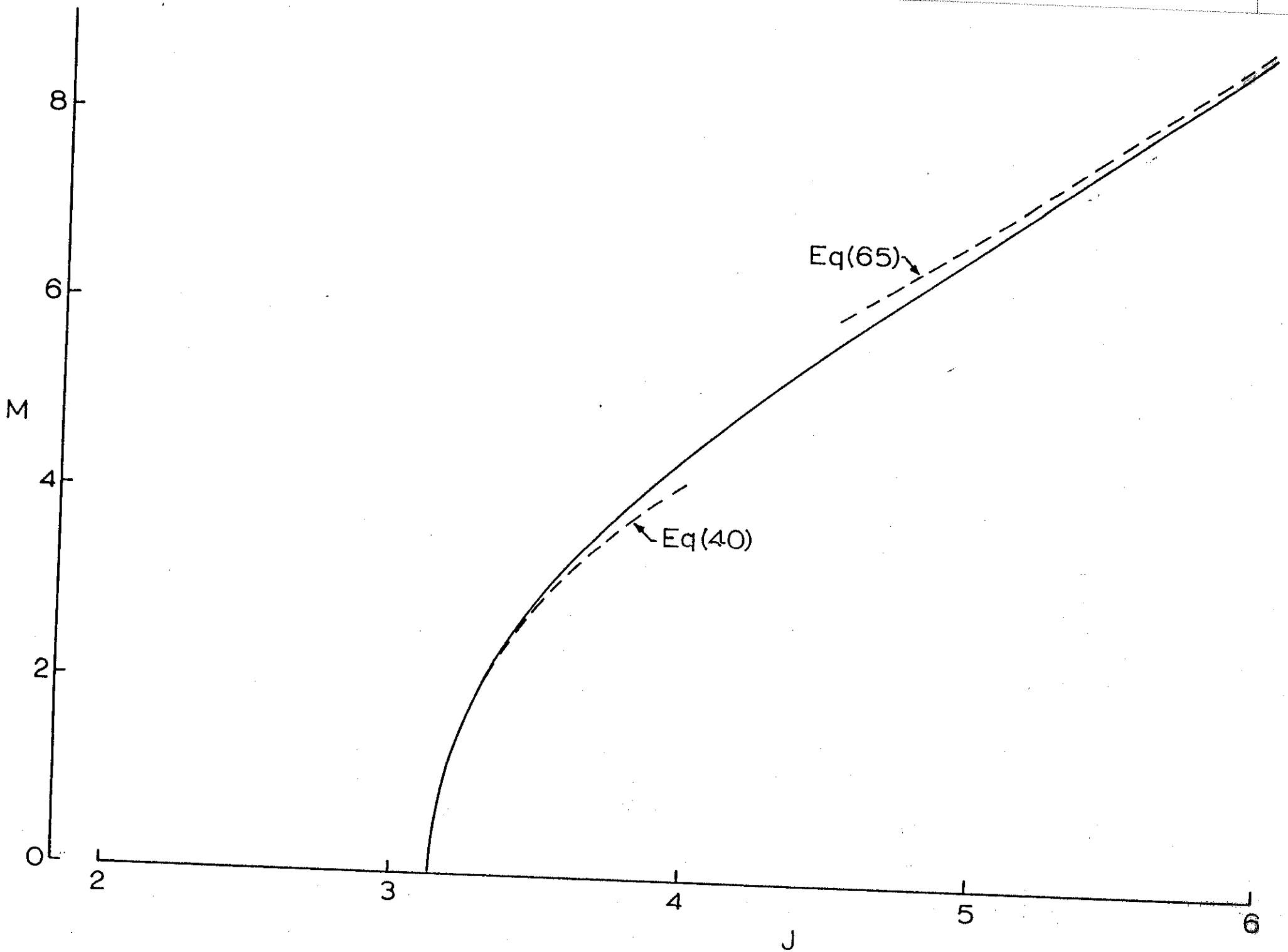

Fig 2

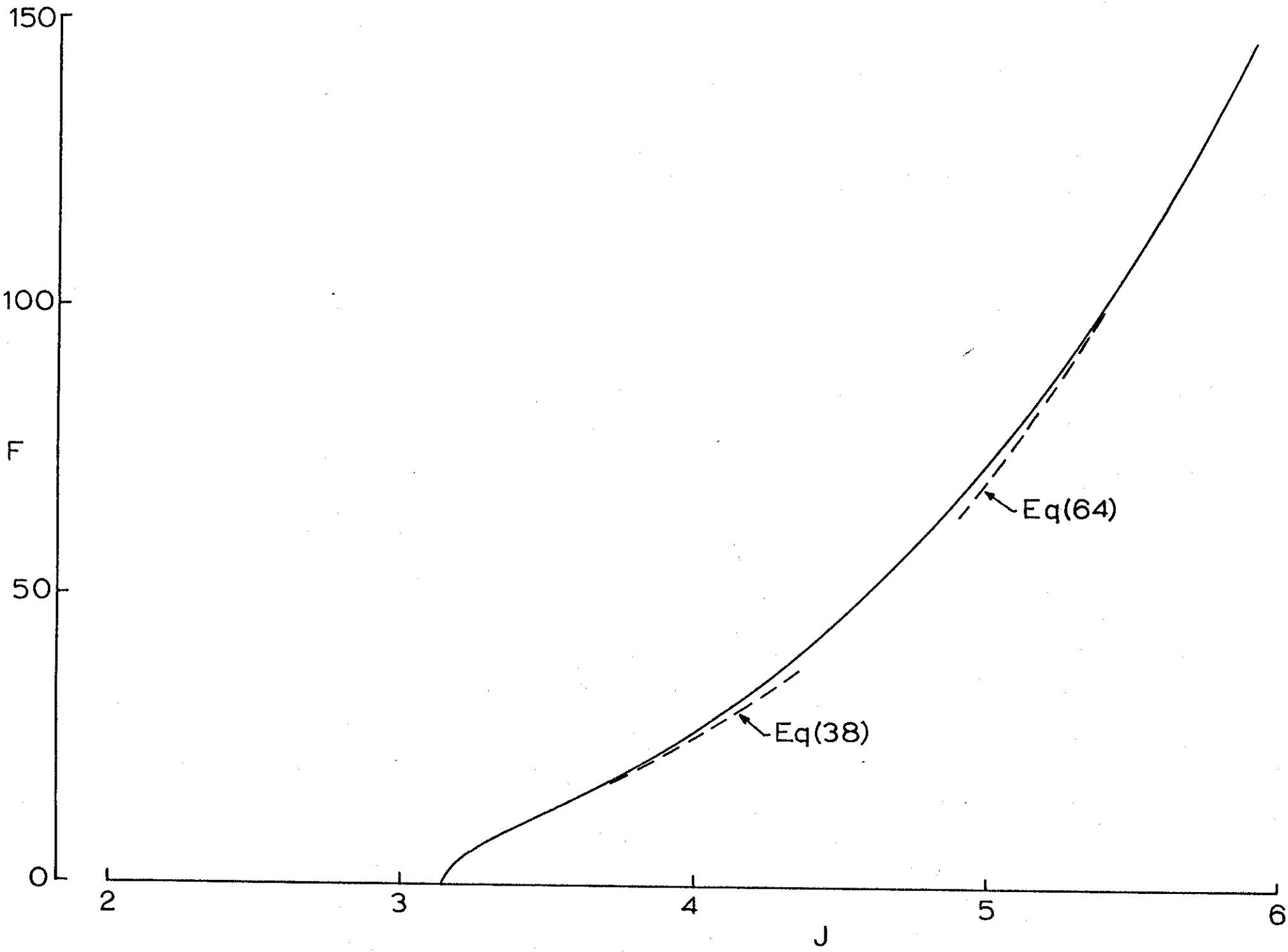

Fig 3

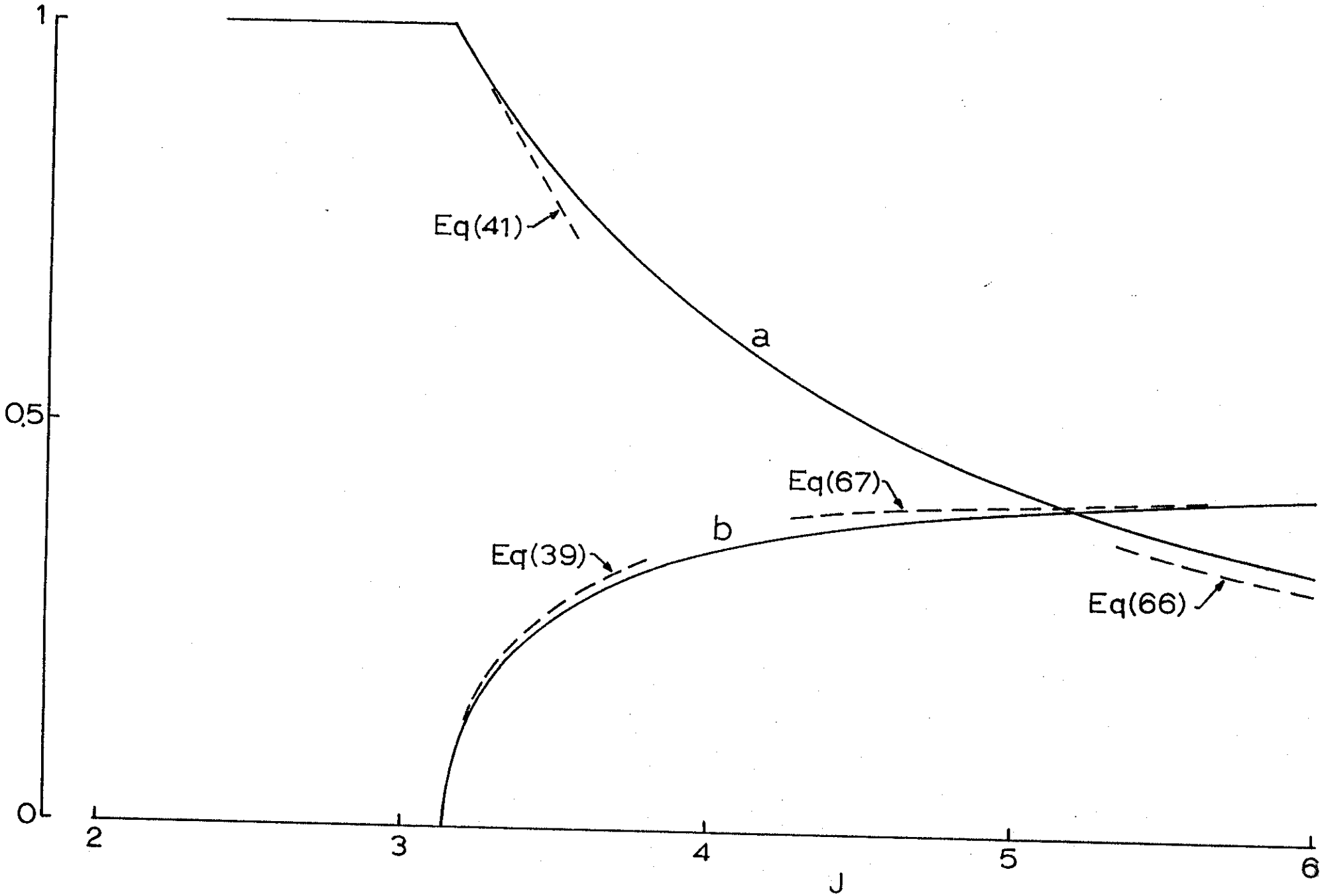

Fig 4

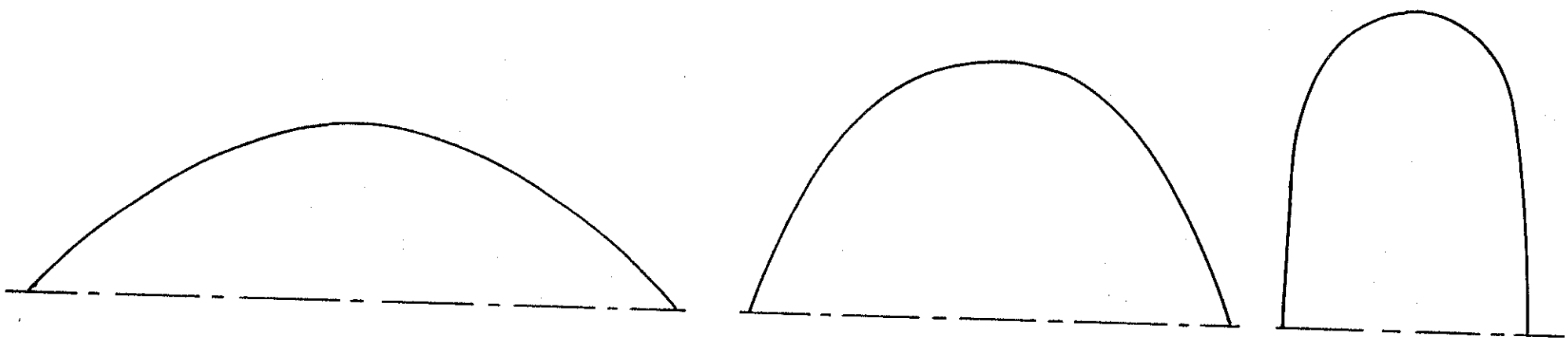

Fig 5